

# RESEARCH MEMORANDUM

AN INVESTIGATION OF THE LIFT, DRAG, AND STATIC-STABILITY

CHARACTERISTICS OF A TRIANGULAR-WING AIRPLANE

CONFIGURATION AT MACH NUMBERS

FROM 3.00 TO 6.28

By Hermilo R. Gloria

Ames Aeronautical Laboratory Moffett Field, Calif.

# NATIONAL ADVISORY COMMITTEE FOR AERONAUTICS

WASHINGTON
December 19, 1956
Declassified January 12, 1961

# RESEARCH MEMORANDUM

AN INVESTIGATION OF THE LIFT, DRAG, AND STATIC-STABILITY CHARACTERISTICS OF A TRIANGULAR-WING AIRPLANE

CONFIGURATION AT MACH NUMBERS

FROM 3.00 TO 6.28

By Hermilo R. Gloria

Ames Aeronautical Laboratory Moffett Field, Calif.

NATIONAL ADVISORY COMMITTEE FOR AERONAUTICS

WASHINGTON
December 19, 1956
Declassified January 12, 1961

#### NATIONAL ADVISORY COMMITTEE FOR AERONAUTICS

## RESEARCH MEMORANDUM

AN INVESTIGATION OF THE LIFT, DRAG, AND STATIC-STABILITY

CHARACTERISTICS OF A TRIANGULAR-WING AIRPLANE

CONFIGURATION AT MACH NUMBERS

FROM 3.00 TO 6.28

By Hermilo R. Gloria

#### SUMMARY

Lift, drag, and static-stability characteristics of a triangular-wing airplane were determined at Mach numbers from 3.00 to 6.28, angles of attack up to 13° at zero sideslip angle, and angles of sideslip up to 8° at zero angle of attack. The test configuration consisted of a triangular wing mounted on a cylindrical afterbody with a fineness-ratio-3 tangent-ogive nose, and a single vertical-tail surface with a trapezoidal plan form. This configuration closely approximates a class of current operational transonic aircraft. Data were also obtained with the basic configuration modified by the addition of a conical flare to the afterbody.

The basic test configuration had values of maximum lift-drag ratios that were comparable to those obtained in previous tests of several airplane configurations designed primarily from considerations of flight at high supersonic speeds.

The longitudinal and directional stability of the basic configuration decreased with increasing Mach number, and resulted in directional instability at the highest test Mach number of 6.28. Addition of the conical flare to the basic configuration increased directional and longitudinal stability as well as lift and drag. Lift-drag ratios, however, were reduced slightly at all but the highest test Mach number.

Impact theory appeared to give adequate estimates of the increment of  $C_{L_{\alpha}}$  and  $C_{m_{\alpha}}$  produced by the addition of conical flare. Estimates of the increment in  $C_{n_{\beta}}$ , however, were somewhat larger than experimental results.

#### INTRODUCTION

Several recent investigations have been devoted to the study of aircraft configurations suitable for flight at high supersonic speeds (see, e.g., refs. 1 to 6). The majority of these configurations have been proposed as either man-carrying aircraft or glide-type missiles, and they have been designed primarily from consideration of their performance and/or heat-transfer characteristics at high supersonic speeds. It is apparent, however, that many of these aircraft, in some part of their flight, must also operate at low speeds and, therefore, their low-speed characteristics are also of interest. To date, however, the bulk of the test effort has been directed to high supersonic speeds and, with a few exceptions (see, e.g., ref. 7), little is known of the low-speed characteristics.

Although some of the configurations proposed are of conventional design, it seems inevitable that at subsonic and transonic speeds many problems will be encountered requiring further study. It would appear, therefore, that a logical alternative to the procedure followed thus far would be to examine the characteristics at high supersonic speeds of configurations which have known low-speed characteristics. In selecting a configuration for study, consideration must still be given to the problems of flight at high supersonic speeds. For example, the leading edges of all planar surfaces should be blunt as required to alleviate local aerodynamic heating. Furthermore, the leading edges should also be highly swept, first, to reduce the drag penalty associated with bluntness and, second, to reduce further the local aerodynamic heating. From these considerations, the triangular-wing airplane appears particularly attractive. One such configuration has been studied in the present investigation.

The wing of the basic test configuration had a 60° triangular plan form mounted on a fuselage of fineness ratio 10. The single vertical fin had a trapezoidal plan form with a blunt leading edge swept back 55°. This configuration, although somewhat simplified, is considered to be sufficiently similar to one class of current operational aircraft with acceptable and well known low-speed and transonic characteristics. The effects of the addition of a conical flare to the fuselage base were also investigated because it was found in reference 4 that such an addition prevented the directional stability of a triangular-wing aircraft from becoming marginal at high supersonic speeds.

#### NOTATION

b wing span

C<sub>A</sub> axial-force coefficient, axial force qS

drag coefficient, drag  $C_{D}$ lift coefficient, lift qS  $C_{L}$ pitching moment about centroid of wing plan area pitching-moment coefficient, .  $C_{m}$  $C_n$ yawing-moment coefficient referred to body axes, yawing moment about centroid of wing plan area qSb side-force coefficient, side force CY increment in lift coefficient due to addition of conical flare ΔCT.  $\Delta C_m$ increment in pitching-moment coefficient due to addition of conical flare  $\Delta C_n$ increment in yawing-moment coefficient due to addition of conical flare <u>-</u> mean aerodynamic chord of wing, including portion submerged in fuselage free-stream Mach number M free-stream dynamic pressure q area of wing, including portion submerged in fuselage, (fig. 1) S angle of attack, deg a. angle of sideslip, deg B

# Subscripts

 $\frac{\partial}{\partial \alpha}$ , per deg

 $\frac{\partial}{\partial \beta}$ , per deg

#### APPARATUS AND TESTS

Tests were conducted in the Ames 10- by 14-inch supersonic wind tunnel, which is described in detail in reference 8. Aerodynamic forces and moments acting on the models were measured with a strain-gage balance. All models were supported from the rear by stings that were shrouded to within 0.04 inch of the model base. Base pressures were measured in all tests and the resultant base forces (referred to free-stream static pressure) were subtracted from the measured total forces. Thus, all data presented are for forces acting on the models ahead of the base.

Principal dimensions of the basic test configuration are shown in figure 1. Views of the test model are also shown in the photographs in figure 2. The model was modified, as indicated by the dashed lines in figure 1, by adding a conical flare at the base. This flare is the frustum of a fineness-ratio-5 cone extending 2.07 body diameters forward of the base and increasing the body base diameter by a factor of  $\sqrt{2}$ . All models were constructed of steel.

Tests were conducted at Mach numbers of 3.00, 4.26, 5.04, and 6.28, angles of sideslip up to 8° at zero angle of attack, and angles of attack up to 13° at zero sideslip angle. The free-stream Reynolds numbers based on the mean aerodynamic chord of the configuration were:

Mach number	Reynolds number, million		
3.00	2.96		
4.26	2.58		
5.04	1.24		
6.28	.54		

Variations in stream Mach number did not exceed  $\pm 0.02$  at Mach numbers from 3.00 to 5.04 and  $\pm 0.04$  at Mach number 6.28. Deviations in free-stream Reynolds number did not exceed  $\pm 50,000$  from the values previously given. The estimated error in angle of attack and angle of sideslip did not exceed  $\pm 0.2^{\circ}$ .

Precision of the experimental results is affected by uncertainties in measurement of forces, moments, and base pressures as well as in the determination of free-stream dynamic pressure and angle of attack or sideslip. These uncertainties resulted in maximum possible errors in the aerodynamic force and moment coefficients as shown in the following table:

Mach number	C <sub>D</sub> , C <sub>A</sub>	$c_L$ , $c_Y$	Cm	Cn
3.00	±0.002	±0.002	±0.004	±0.005
4.26	±.002	±.002	±.004	±.005
5.04	±.002	±.002	±.004	±.005
6.28	±.004	±.004	±.008	±.010

## RESULTS AND DISCUSSION

The variations of lift coefficient with drag coefficient, angle of attack, and pitching-moment coefficient are shown in figure 3. Liftcurve slope,  $C_{L_Q}$ , and static longitudinal stability decrease with increasing Mach number. This decrease is more clearly seen in figure 4, where  $C_{L_{CL}}$  and  $-(dC_m/dC_L)$  for both configurations are presented as a function of Mach number. It is evident that the addition of conical flare increases the longitudinal stability of the configuration, an effect previously noted in reference 4. The lift of the configuration is also increased, and although there is an increase in drag (see fig. 3), there is only a small net decrease in maximum lift-drag ratio of the configuration. This decrease is more clearly shown in figure 5 where maximum lift-drag ratios for both configurations tested are presented as a function of Mach number. Values of maximum lift-drag ratio for the basic configuration range from 4.82 at M = 3.00 to 3.30 at M = 6.28. At Mach numbers from 3.00 to 5.04, addition of base flare reduces these values, but only by about 2 percent. The values of maximum lift-drag ratio for the two configurations are approximately equal at the highest test Mach number. The decrease in maximum lift-drag ratio of both test configurations with increasing Mach number may be attributed, in part, to the increased skin-friction drag associated with the decrease in test Reynolds numbers at the higher test Mach numbers.

Values of maximum lift-drag ratio of a triangular-wing airplane reported in reference 3 are also presented in figure 5 for comparison with the present test results. The reference airplane, designed primarily from considerations of flight at high supersonic speeds, consisted of triangular-wing and -tail surfaces with highly swept leading edges mounted on a cylindrical afterbody with a minimum-drag nose of high fineness ratio. The particular configuration chosen was the most efficient configuration reported in reference 3. It can be seen that at Mach numbers from 3.00 to 5.04, the maximum lift-drag ratios obtained with the reference configuration are from 6 to 20 percent lower than the values obtained with the basic test configuration of the present investigation. At the highest test Mach number, the maximum lift-drag ratios are approximately equal. It is apparent, therefore, that the basic test configuration of the present

NACA RM A56H27

investigation, which closely approximates configurations designed for transonic speeds, will also provide relatively high lift-drag ratios at high supersonic speeds.

The variation of side-force, axial-force, and yawing-moment coefficients with angle of sideslip are presented in figure 6 for both test configurations. There is a marked decrease in side-force and yawingmoment coefficients as the test Mach number is increased. This decrease can be attributed, for the most part, to the expected decrease in verticaltail force with increasing Mach number, and results in directional instability for the basic configuration at the highest test Mach number (fig. 6 (a)). The addition of conical flare to the basic configuration results in an increase in Cy and Cn as shown in figure 6(b), and the modified configuration remains directionally stable throughout the range of Mach numbers tested. The effect of adding the conical flare to the basic configuration is more easily seen in figure 7, where CyB and the directional stability derivative,  $C_{n_{\beta}}$ , (measured at  $\alpha = \beta = 0^{\circ}$ ) are shown as a function of test Mach number for both configurations. It is apparent that the increment of  $C_{n_{\beta}}$  and  $C_{Y_{\beta}}$  provided by the addition of conical flare is essentially independent of Mach number.

A theoretical estimate of the increment in  $C_{L_{\alpha}}$ ,  $C_{m_{\alpha}}$ , and  $C_{n_{\beta}}$  provided by the addition of conical flare has been determined using the impact theory of reference 9 (no downwash or sidewash effects on the flare were considered). The estimates are presented in figure 8 for comparison with experimental values. Impact theory appears to give adequate estimates of the increment of  $C_{L_{\alpha}}$  and  $C_{m_{\alpha}}$  produced by the addition of conical flare. Estimates of the increment in  $C_{n_{\beta}}$ , however, appear to be somewhat larger than experimental results.

### CONCLUSIONS

Lift, drag, and static-stability characteristics of a triangular-wing configuration have been determined at Mach numbers from 3.00 to 6.28, angles of attack up to 13° at zero sideslip angle, and angles of sideslip up to 8° at zero angle of attack. The basic test configuration closely approximates a class of current operational transonic aircraft. Data have also been obtained with the basic configuration modified by the addition of a conical flare to the fuselage base. From the results of these tests, the following conclusions have been drawn:

1. The static longitudinal and directional stability of the basic test configuration decrease with increasing test Mach number, and directional instability results at the highest test Mach number.

- 2. Values of maximum lift-drag ratio for the basic configuration are entirely comparable to those obtained previously with several airplane configurations designed primarily from considerations of flight at high supersonic speeds.
- 3. The addition of conical flare to the basic test configuration increases longitudinal and directional stability as well as lift and drag. The configuration becomes directionally stable throughout the test Mach number range with the addition of the flare. Lift-drag ratios, however, are reduced slightly at all but the highest test Mach number.
- 4. Impact theory appears to give adequate estimates of the increment of  $C_{L_{\alpha}}$  and  $C_{m_{\alpha}}$  produced by the addition of conical flare. Estimates of the increment in  $C_{n_{\beta}}$ , however, appear to be somewhat larger than experimental values.

Ames Aeronautical Laboratory
National Advisory Committee for Aeronautics
Moffett Field, Calif., Aug. 27, 1956

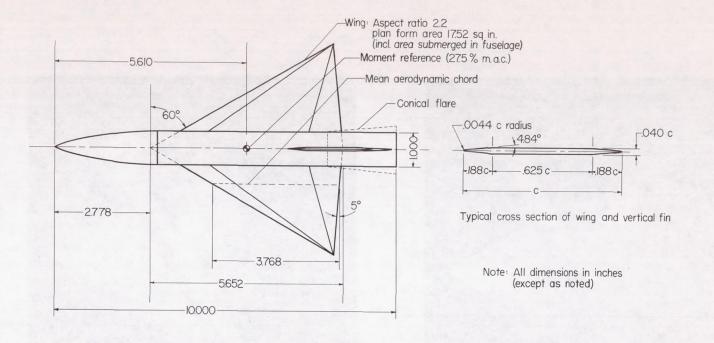
#### REFERENCES

- 1. Penland, Jim A., Ridyard, Herbert W., and Fetterman, David E., Jr.:
  Lift, Drag, and Static Longitudinal Stability Data From an Exploratory Investigation at a Mach Number of 6.86 of an Airplane Configuration Having a Wing of Trapezoidal Plan Form. NACA RM L54L03b, 1955.
- 2. Dunning, Robert W., and Ulmann, Edward F.: Static Longitudinal and Lateral Stability Data From an Exploratory Investigation at Mach Number 4.06 of an Airplane Configuration Having a Wing of Trapezoidal Plan Form. NACA RM 155A21, 1955.
- 3. Neice, Stanford E., Wong, Thomas J., and Hermach, Charles A.: Lift, Drag, and Static Longitudinal Stability Characteristics of Four Airplane-Like Configurations at Mach Numbers From 3.00 to 6.28. NACA RM A55C24, 1955.
- 4. Wong, Thomas J., and Gloria, Hermilo R.: A Preliminary Investigation of the Static Stability Characteristics of Four Airplane-Like Configurations at Mach Numbers From 3.00 to 6.28. NACA RM A56A06, 1956.
- 5. Savin, Raymond C., and Wong, Thomas J.: Lift, Drag, and Static Longitudinal Stability Characteristics of Configurations Consisting of Three Triangular Wing Panels and a Body of Equal Length at Mach Numbers From 3.00 to 6.28. NACA RM A55K21, 1956.

NACA RM A56H27

- 6. Eggers, A. J., Jr., and Syvertson, Clarence A.: Aircraft Configurations Developing High Lift-Drag Ratios at High Supersonic Speeds. NACA RM A55105, 1956.
- 7. Delany, Noel K.: Exploratory Investigation of the Low-Speed Static Stability of a Configuration Employing Three Identical Triangular Wing Panels and a Body of Equal Length. NACA RM A55C28, 1955.
- 8. Eggers, A. J., Jr., and Nothwang, George J.: The Ames 10- By 14-Inch Supersonic Wind Tunnel. NACA TN 3095, 1954.
- 9. Grimminger, G., Williams, E. P., and Young, G. B. W.: Lift on Inclined Bodies of Revolution in Hypersonic Flow. Jour. of Aero. Sci., vol. 17, no. 11, Nov. 1950, pp. 675-690.

X



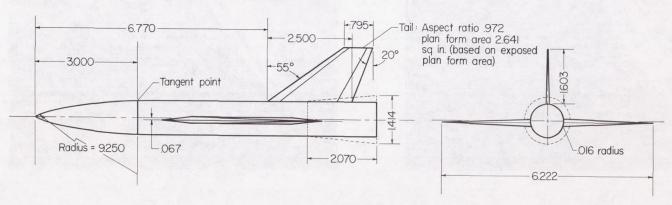
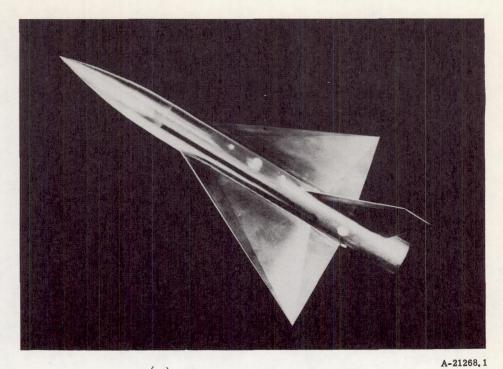
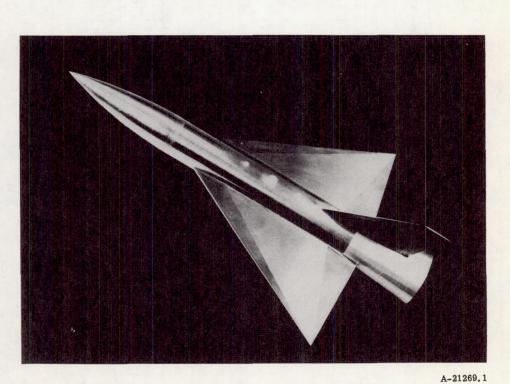


Figure I.- Details of test model.



(a) Basic configuration.



(b) Basic configuration with conical flare.

Figure 2. - Test models.

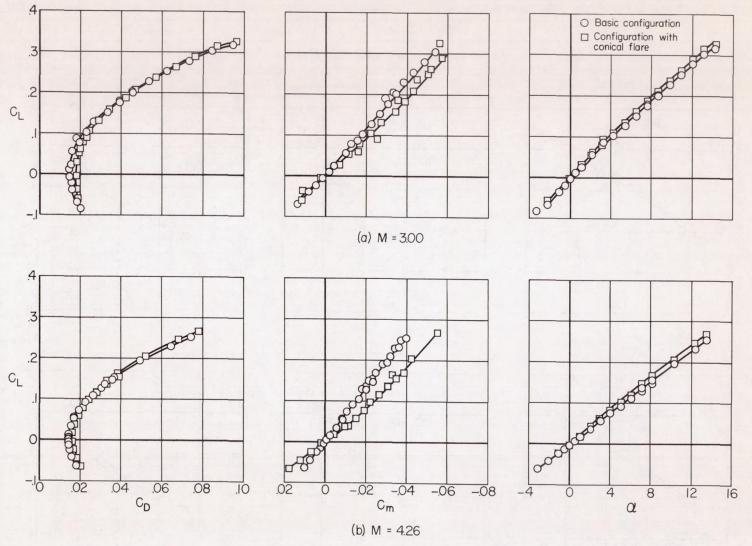


Figure 3.- Lift, drag, and static-longitudinal-stability characteristics.

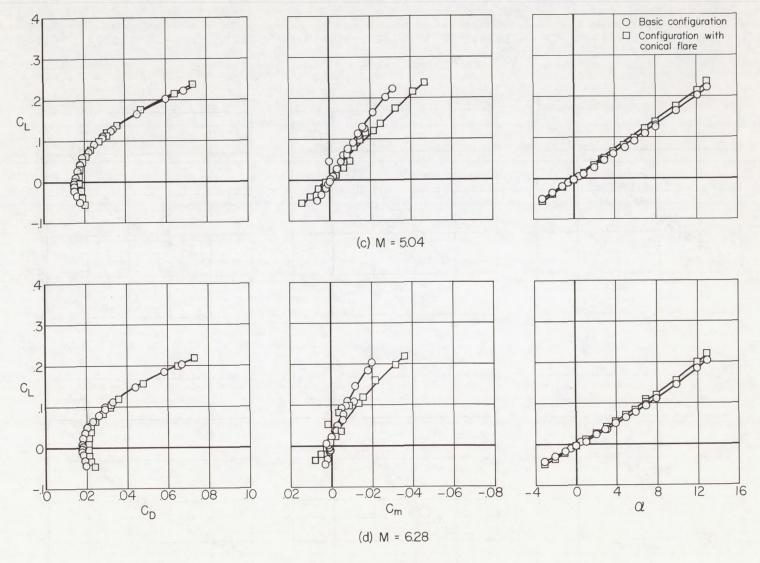


Figure 3.- Concluded.

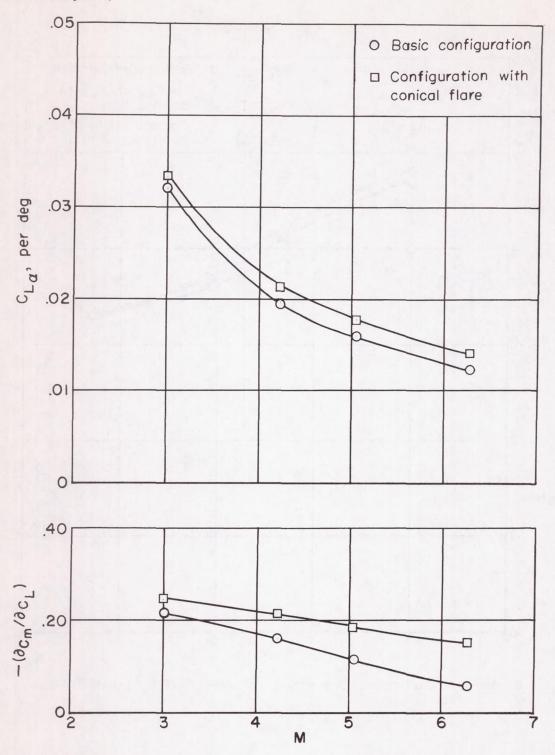


Figure 4.- Variation of lift-curve slope and static longitudinal stability with Mach number ( $\alpha = \beta = 0^{\circ}$ ).

NACA RM A56H27

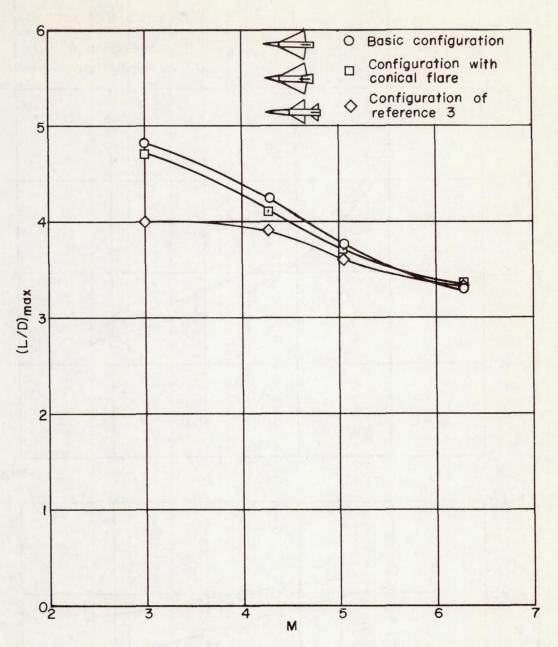


Figure 5. - Variation of maximum lift-drag ratio with Mach number.

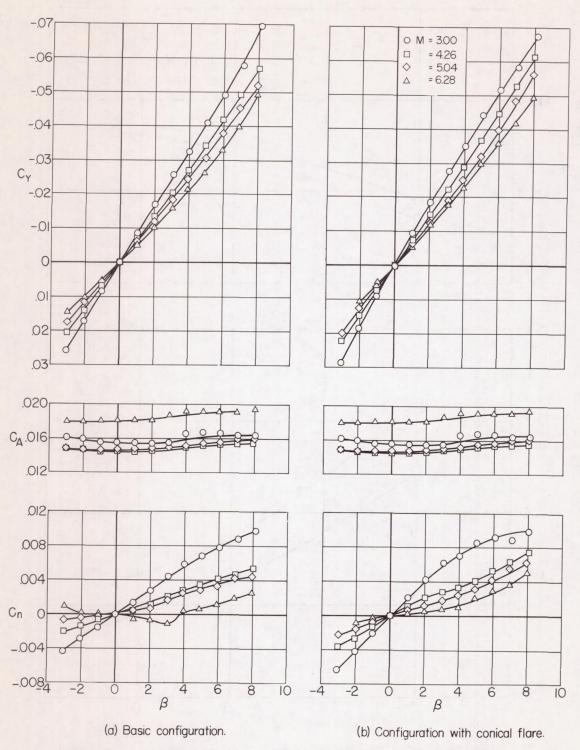


Figure 6.- Variation of side-force, axial-force, and yawing-moment coefficients with angle of sideslip,  $\alpha=0^{\circ}$ .

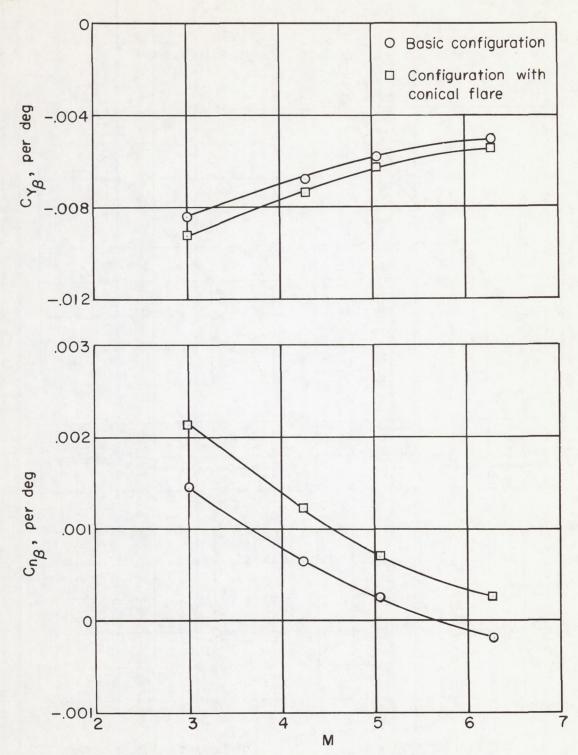


Figure 7.- Variation of side-force-curve slope and directional stability with Mach number (  $\alpha$  =  $\beta$  =  $0^{O}$  ).

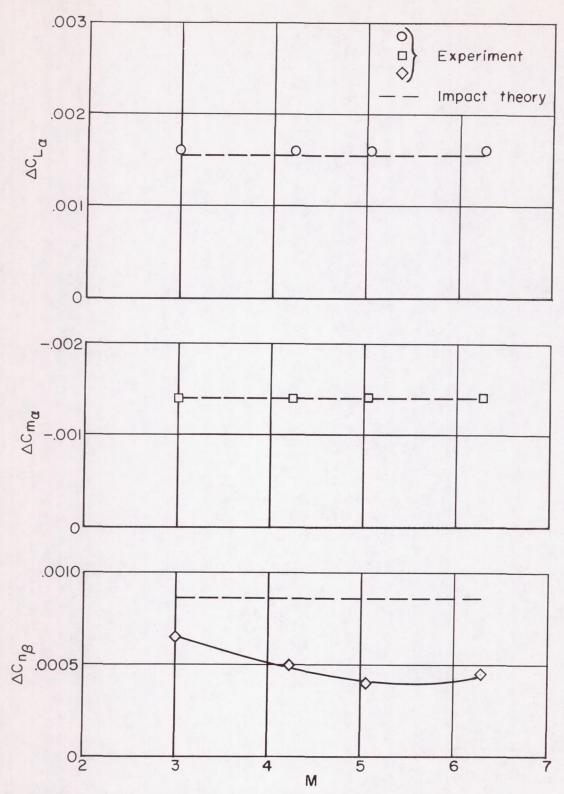


Figure 8.- Comparison of theoretical and experimental values of  $\Delta C_{L_{\alpha}}$ ,  $\Delta C_{m_{\alpha}}$ ,  $\Delta C_{n_{\beta}}$  due to flare ( $\alpha = \beta = 0^{\circ}$ ).

